Atomistic Simulations of Materials

Amogh A

A PROJECT REPORT ON

Atomistic Simulations of Materials

by

Amogh A   2022B5AA0890H

prepared in the partial fulfilment of
BITS F221 - Practice School I

BIRLA INSTITUTE OF TECHNOLOGY AND SCIENCE,
PILANI, HYDERABAD CAMPUS
July, 2024

Declaration of Authorship

I, Amogh A, declare that this document titled, *'Atomistic Simulations of Materials'* and the work presented in it are my own. I confirm that:

- this work was done wholly or mainly while in candidature for the study project course BITS F221 at this university.

- where any part of this work has previously been submitted for a degree or any other qualification at this university or any other institution, this has been clearly stated.

- where I have consulted the published work of others, this is always clearly attributed.

- where I have quoted from the work of others, the source is always given. With the exception of such quotations, this report is entirely my own work.

- I have acknowledged all main sources of help.

- where the thesis is based on work done by myself jointly with others, I have made clear exactly what was done by others and what I have contributed myself.

Signed: Amogh A

_____

Date: 18$^{\text{th}}$ July, 2024

_____

Contents

List of Figures

List of Tables

Early Quantum Mechanics

1.1. The Method

In quantum mechanics, any possible measurable information about a given quantum system is contained in the system's wave function $\Psi(\mathbf{r}, t)$. Granted that we know the potential function, I can solve for the wave function using the SE

$$i\hbar\frac{\partial\Psi(\mathbf{r}, t)}{\partial t} = \left(\frac{i^2\hbar^2}{2m}\nabla^2 + V\right)\Psi(\mathbf{r}, t).$$

1.2. The Problem

This equation can be solved in closed form for only a handful of simple potential functions. Infinite square well, harmonic oscillator and hydrogen-like atoms are a few examples, but one does need to know the properties of systems which are arguably more complex. It is not possible to solve for the wave function of an electron in a crystalline lattice in closed form and expect to understand its behaviour from there. The fundamental difference lies in the number of interacting entities. In a crystal, a free electron is under the influence of a *large* number of nuclei not to mention other electrons, and external electric and/or magnetic potentials. The problem of solving the SE now becomes very complicated. Thus, other methods have to be employed to solve the problem at hand. We shall discuss a few approaches to solving the N-body problem chronologically and apply the techniques to understand the behaviour of some simple yet exciting systems like graphene and silicon.

2

The Thomas-Fermi Model

2.1. The Statistical Approach

One of the first attempts to understand the many-body problem was made by Llewellyn Thomas and Enrico Fermi who independently proposed their semi-classical statistical model of many-body interacting systems[2, 22].

Consider the electrons in an atom as a continuous charge distribution rather than as individual particles. Let the space around an atom be divided into small cubes of side l and volume $\Delta V = l^3$ such that each cube contains a fixed number of electrons ΔN. Though different cells may have different numbers of electrons, it is important to note that electrons in other cells are assumed to be independent, non-interacting fermions.

In a three-dimensional infinite square well, the energy levels of a particle are given by

$$\varepsilon(n_x, n_y, n_z) = \frac{h^2}{8ml^2}(n_x^2 + n_y^2 + n_z^2)$$

$$\varepsilon(n_x, n_y, n_z) = \frac{h^2}{8ml^2}R^2.$$

For large values of R, the number of distinct energy levels with energies smaller than ε can be approximated as

$$\Phi(\varepsilon) = \frac{1}{8}\left(\frac{4\pi R^3}{3}\right) = \frac{\pi}{6}\left(\frac{8ml^2\varepsilon}{h^2}\right)^{3/2}.$$

The total kinetic energy of an electron in a cell is calculated by summing the contributions

from different energy states

$$\Delta E = 2 \int \varepsilon f(\varepsilon) g(\varepsilon) \, d\varepsilon \tag{2.1}$$

$$\Delta E = \frac{8\pi}{5} \left(\frac{2m}{h}\right)^{3/2} l^3 \varepsilon_F^{5/2} \tag{2.2}$$

$$\Delta E = \frac{3h^2}{10m} \left(\frac{3}{8\pi}\right)^{2/3} l^3 \left(\frac{\Delta N}{l^3}\right)^{5/3} \tag{2.3}$$

where $f(\varepsilon)$ is the Fermi distribution, $g(\varepsilon)$ is the number of levels between ε and $\varepsilon + \delta\varepsilon$ and ε_F is the Fermi energy. The complete derivation of the above equations can be found in McQuarrie [14].

The total kinetic energy is now a functional of the electron density $\rho = \Delta N / l^3$, which in atomic units is

$$T_{TF}[\rho] = C_F \int \rho^{5/3}(\mathbf{r}) \, d\mathbf{r}.$$

It is crucial to note that this is where we first encounter *local density approximation* where the electronic properties are determined by a functional of electron density which assumes that within the unit cell, the electron density can be safely assumed to be a constant.

If we thus ignore the exchange and correlation terms and only assume the *classical* electrostatic energies – attractive nucleus-electron and repulsive electron-electron interaction, the total energy can be written as

$$E_{TF}[\rho] = T_{TF}[\rho] - Z \int \frac{\rho(\mathbf{r})}{|\mathbf{r}|} \, d\mathbf{r} + \frac{1}{2} \iint \frac{\rho(\mathbf{r}_1)\rho(\mathbf{r}_2)}{|\mathbf{r}_1 - \mathbf{r}_2|} \, d\mathbf{r}_1 \, d\mathbf{r}_2.$$

Let N be the total number of electrons in the atom. If

$$N = N[\rho(\mathbf{r})] = \int \rho(\mathbf{r}) \, d\mathbf{r},$$

and we assume that the ground state electron density minimises the total energy functional $E_{TF}[\rho(\mathbf{r})]$, we can solve for $\rho(\mathbf{r})$ using the above equation as a constraint on the energy equation. The iterative process of guessing a ground state $\rho(\mathbf{r})$ and checking if its energy is the lowest guarantees that for some $\rho(\mathbf{r})$, we will get the lowest energy.

If $\phi(\mathbf{r})$ is the electrostatic potential for a given $\rho(\mathbf{r})$, then

$$\frac{d^2\phi(\mathbf{r})}{dr^2} = \frac{4\pi e^2}{a_0} \left(\frac{2m}{\hbar^2}\right)^{3/2} \phi^{3/2}(\mathbf{r}).$$

Thus, we have, for the first time, a *solution* to the many-body quantum problem.

2.2. The Problem

Because so many assumptions went into the construction of this model, it has major limitations. For one, electrons are not a continuous fluid and can only be in certain allowed energy states. This model also fails to account for the exchange and correlation energies of the electron and thus is an incomplete picture. Electrons are fermions and are thus only accurately described by an anti-symmetric wave function. By failing to account for this, Pauli's exclusion principle is thrown out. The electrostatic potential is overly simplified and fails to describe the behaviour of electrons near the nucleus and high electron density – like near bonds. Edward Teller showed that this model can never be used to describe a molecule as its energy will always be greater than the sum of its constituents[21].

<div align="right">

3

</div>

Hartree's Model

3.1. Hartree Model

In 1927, the English mathematician Douglas Hartree developed a novel mathematical approach to solve the many-body problem using numerical analysis[7]. He wanted to do away with empirical parameters to solve many-body-time-independent Schrödingerequation, an approach now called *ab initio*. His method is now known as the Hartree method or *Hartree product*.

Hartree knew that the wave function which describes all the electrons, Ψ, is very complex to calculate directly. So, he first calculated the solutions to the Schrödingerequation for individual electrons $1, 2, \ldots, n$ in the states $\alpha, \beta, \ldots, \pi$: $\psi_\alpha(\mathbf{x}_1), \psi_\beta(\mathbf{x}_2), \ldots, \psi_\pi(\mathbf{x}_n)$. He then argued that since each ψ is a solution to the Schrödingerequation, their product must at least be an approximate solution. The product of all the ψs is called the *Hartree product*:

$$\Psi(x_1, x_2 \ldots, x_n) = \psi_\alpha(\mathbf{x}_1)\psi_\beta(\mathbf{x}_2) \ldots \psi_\pi(\mathbf{x}_n).$$

The total energy of the system is described by the Hamiltonian operator which includes the kinetic and interaction energies of the particles. It is given by:

$$\hat{H} = -\frac{\hbar^2}{2m}\sum_i \nabla^2_{r_i} + \frac{1}{2}\sum_{i \neq j} \frac{e^2}{4\pi\varepsilon_0|\mathbf{r}_i - \mathbf{r}_j|} - \sum_i \frac{Ze^2}{4\pi\varepsilon_0|\mathbf{r}_i|}$$

where N is the number of electrons and $\mathbf{r}_i$ is the position of the ith particle. Like the Thomas-Fermi model, this model also assumes that the particles are independent. This is known as the *mean field approximation*. This method is the unsymmetrized version of the Slater determinant in the later Hartree-Fock method[**Slater'sPaper**].

In the *Hartree approximation*, the electron-electron interaction is approximated by replacing the actual term with an average interaction term of all the electrons. The

electron-electron interaction term $V(\mathbf{r}_i - \mathbf{r}_j)$ is replaced by the mean-field term

$$V_{mean}(\mathbf{r}_i) = \int \frac{n(r)_j}{|\mathbf{r}_i - \mathbf{r}_j|} \, d\mathbf{r}_j$$

where $n(\mathbf{r}_j)$ is the electron density at $\mathbf{r}_j$.

Hartree's method was shown to not respect the fermionic nature of electrons [19, 3]. This approach also ignores the exchange term of the electrons and thus gives a rough image. Also, since the Hartree method treats the electron independently in an averaged-out potential, it neglects the correlation beyond the mean field.

The algorithm to solve for the electron density is as follows:
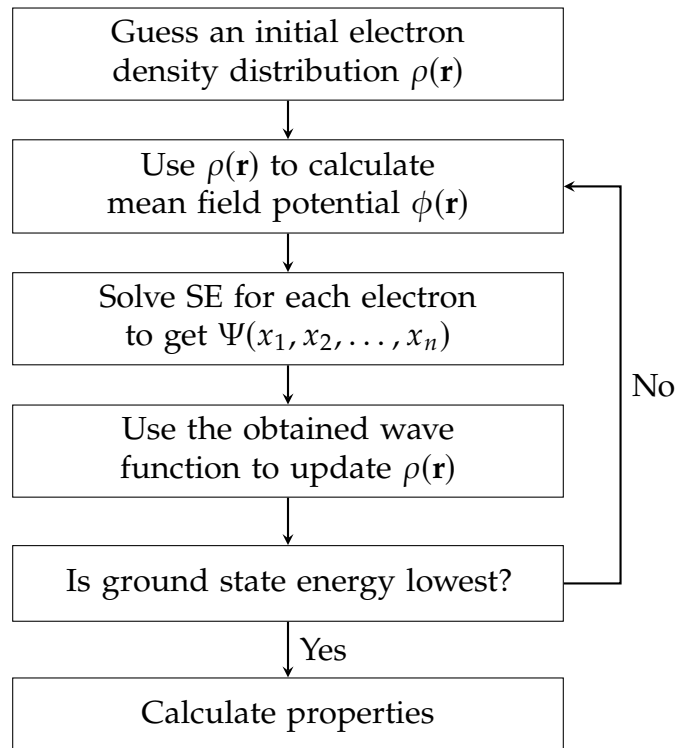
Figure 3.1: Hartree Algorithm

4

The Hartree-Fock Model

4.1. Hartree-Fock Model

The previously stated Hartree method can be viewed as an approximation of the Hartree-Fock (HF) method by neglecting the exchange parameters. Vladimir Fock's original method to solve the many-body problem relied heavily on group theory which became too abstract for contemporary physicists. In 1935, Hartree reformulated his approach to be suitable for computation [8].

The HF method makes 5 major simplifications:

1. The Born-Oppenheimer approximation is a mathematical approximation which states that since the mass of the nuclei is much larger than that of the electrons, they move much slower than the electrons and thus their wave functions can be treated separately. The complete wave function is a function of the nuclear and electronic coordinates.

2. Relativistic effects are completely neglected.

3. The energy eigenfunction is assumed to be describable by a single Slater determinant which takes care of the fermionic nature of the electrons.

4. The HF is another instance of the MFA and thus neglects the Coulomb correlation.

5. The variational solution is assumed to be a linear combination of the finite number of orthogonal basis functions.

The Slater determinant is a device which is an antisymmetrised product of N orthonormal spin orbitals $\psi_i(\mathbf{x})$:

$$\Psi(\mathbf{x}) = \frac{1}{\sqrt{N!}} \begin{vmatrix} \psi_1(x_1) & \psi_2(x_1) & \ldots & \psi_N(x_1) \\ \psi_1(x_2) & \psi_2(x_2) & \ldots & \psi_N(x_2) \\ \psi_1(x_3) & \psi_2(x_3) & \ldots & \psi_N(x_3) \\ \vdots & \vdots & \ddots & \vdots \\ \psi_1(x_N) & \psi_2(x_N) & \ldots & \psi_N(x_N) \end{vmatrix} \cdot$$

4.2. Variational Principle on Ground State

The energy of a system whose wave function is Ψ is

$$E[\Psi] = \frac{\langle \Psi | \hat{H} | \Psi \rangle}{\langle \Psi | \Psi \rangle}.$$

Since each particular measurement of E gives one of the eigenvalues of $\hat{H}$, we have

$$E[\Psi] \geq E_0.$$

The Hartree-Fock energy is an *upper bound* to the actual ground state energy of the system. It is also the minimal energy as predicted by a single Slater determinant.

Every eigenstate of the wave function is an extremum of the functional $E[\Psi]$. Thus, we can replace SE by the variational principle

$$\delta E[\Psi] = 0.$$

The starting point for the HF method is a set of approximate single-electron wave functions known as *spin-orbitals*. For atomic orbital calculations, these are usually hydrogen-like atoms with appropriate nuclear charge and for molecular orbital calculations, they will be LCAO.

4.3. The Fock Operator

The Fock operator is truly a matrix, the Fock matrix. It is given by

$$\hat{F}(i) = \hat{H}(i) + \sum_{j=1}^{N} [\hat{J}_j(i) - \hat{K}_j(i)],$$

where:

$\hat{H}(i)$ is the usual Hamiltonian,

$\hat{J}_j(i)$ is the Coulomb operator, defining the repulsive force between the jth and ith

electrons,

$\hat{K}_j(i)$ is the exchange operator, which takes care of the quantum effects produced by swapping two electrons.

The Fock matrix takes the orbitals as input to construct the Fock matrix and the eigenfunctions of the Fock operator are in turn new orbitals which can be used to construct a new Fock matrix. This iterative process can be repeated until the change in electronic energy of the ground state in successive iterations falls below an acceptable value. The famous Hartree-Fock equation is thus

$$\hat{F}\psi_i(\mathbf{x}) = \sum_{j=1}^{N} \varepsilon_{ij}\psi_i(\mathbf{r}).$$

The HF method can be summarised in this flowchart:
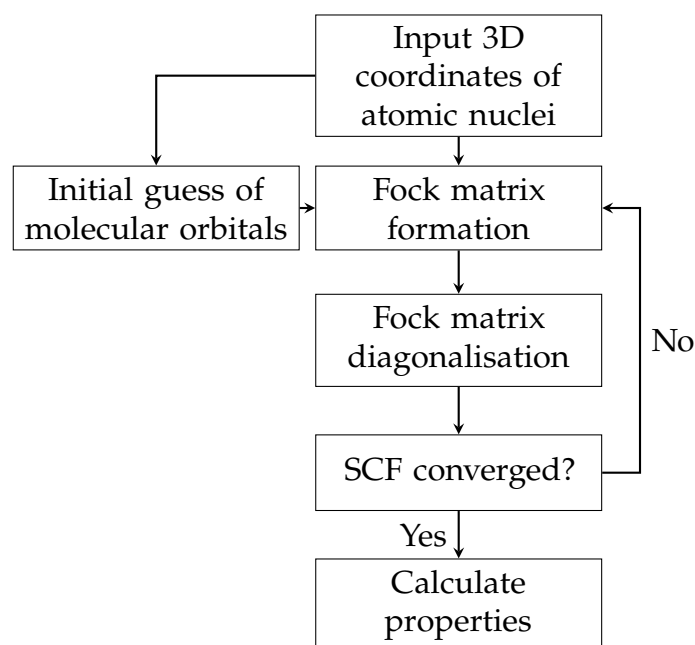
Figure 4.1: Hartree-Fock Algorithm

This method too had significant flaws. For one, this too did not account for the electron correlation beyond MFA. This resulted in the inaccurate physical description of short-range phenomena. The MFA itself thus gave only a rough estimate of ground reality. The "true" wave function of the N-body system is never a single Slater determinant. For systems which involve bond-breaking or excited states, a single Slater determinant is insufficient. The stability of closed-shell systems (example: Noble gas configuration – Kr, Zn^{2+}) is overestimated while those of open-shell systems (example: Radicals with unpaired electrons) are underestimated. While constructing the Fock operator ($\hat{F}$), the spin of the electron was neglected. Thus certain magnetic properties of polarised systems can't be calculated. Moreover, this method is computationally expensive. For large systems, which is mostly the case in the real world, its Big O notation is $O(n^4)$.

Note on Electron Correlation

5.1. What is Electron Correlation?

Electrons in a crystal are in constant motion. The correlation energy as described in DFT is the part of the total electronic energy that accounts for the dynamic interactions beyond what can be captured by HF.

1. Total Energy (E_{total}): Exact ground state energy of the many-body interacting system.

2. Hartree-Fock energy (E_{HF}): Energy obtained by HF method which is approximately correct. It accounts for exchange but not the correlation of electrons.

3. Correlation Energy (E_{corr}): The difference between exact total energy and HF energy:
$$E_{corr} = E_{total} - E_{HF}.$$

In DFT, the energies are a functional of electron density $\rho(\mathbf{r})$. In DFT, E_{total} is

$$E_{total}[\rho] = T_s[\rho] + E_{ext}[\rho] + E_H[\rho] + E_{xc}[\rho]$$

where:

$T_s[\rho]$ is the kinetic energy of a non-interacting system with the same density,

$E_{ext}[\rho]$ is the energy due to external potential (example: nuclei),

$E_H[\rho]$ is the classical Hartree electrostatic electron-electron repulsion energy:

$$V_H(\mathbf{r}) = \int \frac{\rho(\mathbf{r}')}{|\mathbf{r} - \mathbf{r}'|} \, d^3\mathbf{r}',$$

$E_{xc}[\rho]$ is the exchange-correlation energy functional. The exchange-correlation is

further broken down into

$$E_{xc}[\rho] = E_x[\rho] + E_c[\rho]$$

where $E_x[\rho]$ is the exchange energy, which accounts for the exchange interactions between the electrons and

$E_c[\rho]$ is the correlation energy, which accounts for the dynamic correlation between electron movements.

Dynamic Correlation between Electron Movements: Consider a H_2 molecule. Near the bond, the electron density is considerable. Thus, the electrons actively avoid each other (due to mutual Coulomb repulsion) in that region in very short time scales. Thus, the dynamic correlation term becomes important when dealing with energetic molecules.

Static (Non-Dynamic) Electron Correlation: This arises when the MFA fails to account for the correct electronic configuration due to near-degeneracy or strong interactions between multiple configurations. This becomes significant in transition metal complexes or bond-breaking processes.

6

Density Functional Theory

6.1. Density Functional Theory

Density functional theory finds its origins in the Thomas-Fermi model and was put on concrete theoretical footing by Walter Kohn and Pierre Hohenberg in their framework of the **Hohenberg-Kohn theorems**[9, 11]. The non-relativistic time dependent many body Schrödingerequation is given by

$$\hat{H}\Psi = [\hat{T} + \hat{V} + \hat{U}]\Psi = \left[\sum_{i=1}^{N} \left(\frac{i^2\hbar^2}{2m_i}\nabla_i^2 + V(\mathbf{r}_i) \right) + \sum_{i<j} U(\mathbf{r}_i, \mathbf{r}_j) \right] \Psi$$

There are many specialised methods to solving the above equation based on the expansion of Slater determinants but as previously stated, they are very expensive computationally.

In DFT, the main focus is on the ground state electron density $n(\mathbf{r})$. It allows us to take the many-body problem with $\hat{U}$ to a single-body problem without it. When normalised, $n(\mathbf{r})$ is

$$n(\mathbf{r}) = N \iiint \cdots \int \Psi^*\Psi \, d^3\mathbf{r}_1 \ldots d^3\mathbf{r}_N$$

This relation is reversible: for a given ground state $n(\mathbf{r})$, one can find out the corresponding $\Psi_0(\mathbf{r})$. Thus, Ψ is a unique *functional* of $n(\mathbf{r})$.

$$\Rightarrow \Psi_0 = \Psi[n_0]$$

6.2. Hohenberg-Kohn Theorems

Theorem 1 *The ground state expectation value of any observable $\hat{O}$ is a functional of the ground state electron density, $n(\mathbf{r}_0)$.*

$$\boxed{O_0 = O[n_0] = \langle \Psi[n_0] | \hat{O} | \Psi[n_0] \rangle} \tag{6.1}$$

Theorem 2 *The density which minimises the total energy is the exact ground state energy.*

$$\boxed{E_{v,0} = E_v[n_0] = \langle \Psi[n_0]| \, \hat{H} \, |\Psi[n_0]\rangle}$$

$$E_v[n_0] \le E_v[n']$$

The usual quantum mechanical approach to Schrödingerequation can be summarised as

$$v(\mathbf{r}) \overset{\text{SE}}{\implies} \Psi(\mathbf{r}_1, \mathbf{r}_2 \dots \mathbf{r}_N) \xrightarrow{\langle \Psi| \dots |\Psi\rangle} \text{observables.}$$

But with DFT, the approach is almost flipped on its head:

$$n(\mathbf{r}) \implies \Psi(\mathbf{r}_1, \mathbf{r}_2 \dots \mathbf{r}_N) \implies v(\mathbf{r}).$$

E_v can also be written as

$$E_v[n] = T[n] + U[n] + V[n] = F[n] + V[n]$$

$$V[n] = \int n(\mathbf{r})v(\mathbf{r}) \, d^3 r$$

6.3. Representability Problems

6.3.1. N-representability Problem

This simply states: Given an arbitrary $n(\mathbf{r})$, how does one know that it can be written in the form of the integral equation, an anti-symmetric N-body wave function? This is an important question to ask as if one does numerically find an $n(\mathbf{r})$ which minimises the ground state energy but is *not* N-representable, then it can not be a physical solution. Luckily, for a single-particle density, this problem has been solved: any non-negative function can be written in terms of some anti-symmetric Ψ in the form of the integral equation[4, 6].

6.3.2. v-Representability Problem

This states: Given that a function can be written as the integral equation, how does one know that this is the ground state density for the local potential $v(\mathbf{r})$? This remains to be solved. The Hohenberg-Kohn theorem guarantees that there can never exist *more than one* potential for a given density but it does not exclude the possibility of no potential capable of producing it.

6.4. The Kohn-Sham Equations

As we saw in the Thomas-Fermi model, the oversimplifications led to a loss of accuracy. We traded accuracy for simplicity. But can we do better? This was the same question Walter Kohn and Lu Sham were asking in 1965. They came up with an ingenious

way to calculate the kinetic energy functional. The basis for these equations is the Hohenberg-Kohn theorems[1].

The exact form of the functional which minimises the total energy of the system is usually unknown. The Kohn-Sham approach is to approximate this functional. The key idea is to introduce a set of non-interacting electrons that have the same ground state electron density as the given system. Then use the Kohn-Sham equations to find the density.

1. Express the electron density in terms of a set of single-particle wave functions known as the Kohn-Sham orbitals ($\psi_i(\mathbf{r})$):

$$\rho(\mathbf{r}) = \sum_{i=1}^{N} |\psi_i(\mathbf{r})|^2.$$

2. The Kohn-Sham orbitals are the solutions to the following set of equations

$$\left[\frac{i^2 \hbar^2}{2m} \nabla^2 + V_{eff}(\mathbf{r}) \right] \psi_i(\mathbf{r}) = \varepsilon_i \psi_i(\mathbf{r})$$

Here, ε_i are the Kohn-Sham eigenvalues and $V_{eff}(\mathbf{r})$ is the effective potential given by

$$V_{eff}(\mathbf{r}) = V_{ext}(\mathbf{r}) + V_H(\mathbf{r}) + V_{xc}(\mathbf{r})$$

where the symbols have the usual meaning (see electron correlation).

The algorithm for Kohn-Sham DFT is as follows:
This method **finally** accounts for the exchange-correlation energy of the electron. The exchange-correlation potential is derived from the exchange-correlation functional:

$$V_{xc}[\mathbf{r}] = \frac{\delta E_{xc}[\rho]}{\delta \rho(\mathbf{r})}.$$

Since the exact form of $E_{xc}[\rho]$ is not usually known, LDA or GGA are used in practice.

6.5. Pseudopotentials

The concept of pseudo-potentials was first introduced by Enrico Fermi in 1935 and Hans Hellmann in 1936 [1, 18]. All the electrons in an atom are not equally significant. In a many-electron atom, the electrons can be divided into valence and inner core electrons. The inner core electrons are strongly bonded to the nucleus and do not participate in chemical reactions. They also slightly shield the outer electrons from the nucleus. The valence electrons are the ones which actively participate in the chemical reactions and bond formation/breaking. Thus, the atom can be approximated as an ionic core with valence electrons. When the valence electrons are treated explicitly, the valence

---

[1]Walter Kohn received the 1998 Nobel Prize in Chemistry "for his development of the density functional theory."
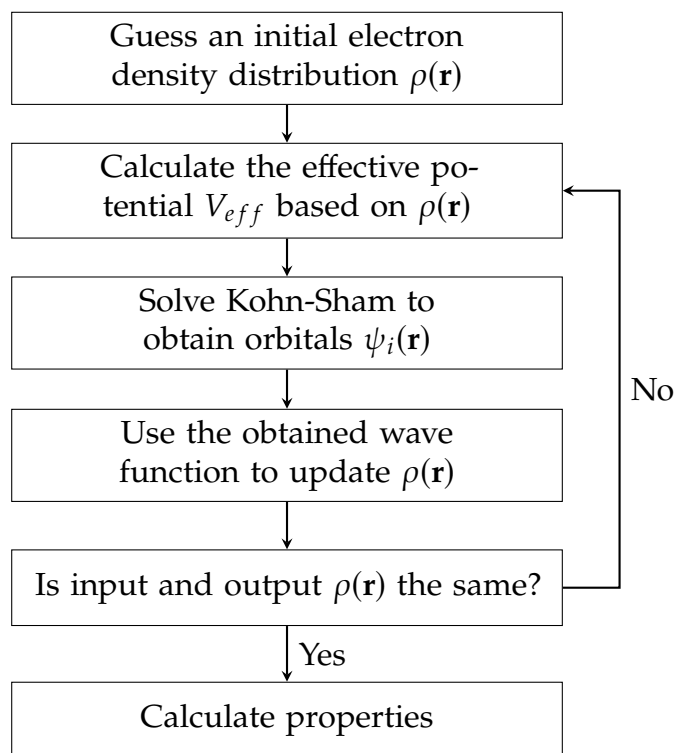
Figure 6.1: Density Functional Theory Algorithm

wavefunctions no longer oscillate rapidly near the core and ensure orthogonality, thus, converging in fewer plane waves making the overall calculation less computationally expensive. Therefore, using pseudo-potentials, a complex system can be simplified without much loss of information.

Though very powerful, DFT too has some limitations:

1. Exchange-correlation approximation errors: Since the exact form of E_{xc} is not known, approximations like LDA or GGA introduce significant errors.

2. Van der Waals Interactions: Standard DFT fails to capture dispersion interactions which are important in molecular crystals, biological systems or certain solutions.

3. Strongly Correlated Systems: The single-determinant approach fails to account for strong electron correlation. Thus, certain properties of transition metal complexes are poorly described.

4. Time-Dependent Systems: Standard DFT is not well suited for time-dependent systems like excited state properties or charge-transfer reactions.

5. Computational Cost: While being more efficient than HF or post-HF models, high accuracy needs large computational resources.

Despite all these limitations, DFT finds applications in condensed matter physics, chemistry, nanotechnology, biochemistry, materials science and surface and catalytic chemistry.

7

Introduction to Solid State Physics

7.1. The Basics

Condensed matter physics deals with studying microscopic and macroscopic properties of matter, mainly in solid and liquid states, which arise due to the electromagnetic interaction between the atoms and electrons. Solid state physics, a branch of condensed matter physics, deals with rigid matter and forms the theoretical basis for materials science and semiconductor electronics.

7.2. The Unit Cell and Bravais Lattices

The properties of most solids can be understood by studying their building blocks – the unit cell. A unit cell can comprise a single atom or a collection of atoms of one or more elements. Understanding the properties of a unit cell reveals a lot about the solid as a whole. In crystallography, there are 14 types of unit cells called Bravais lattices. Any crystalline solid can be represented as a repeating entity of one of these 14 lattices as this arrangement gives the system the lowest possible energy. Ideally, a crystal should not have any grain boundaries or impurities in it. While the size of a unit cell is on the order of a few angstroms, we usually consider crystals to be on the order of millimetres or centimetres. The periodic arrangement of atoms in a crystal can be experimentally verified using techniques like X-ray diffraction. Other experimental techniques like ^{1}H-NMR and ^{13}C-NMR, and FTIR are employed to give us more information about the composition and vibrational frequencies of the solid.

7.3. Bloch's Theorem

Theorem 3 *The solutions to the Schrödinger equation in a periodic potential can be expressed as plane waves modulated by periodic functions.*

Named after the Swiss Nobel laureate Felix Bloch, mathematically this can be written as

$$\psi(\mathbf{r}) = e^{i\mathbf{k}\cdot\mathbf{r}}u(\mathbf{r})$$

where $\mathbf{r}$ is position, ψ is the wave function, u is a periodic function with the same periodicity as the crystal, and the wave vector $\mathbf{k}$ is the crystal momentum vector. Functions of this form are known as Bloch functions and serve as the set of bases for electrons in crystalline solids.

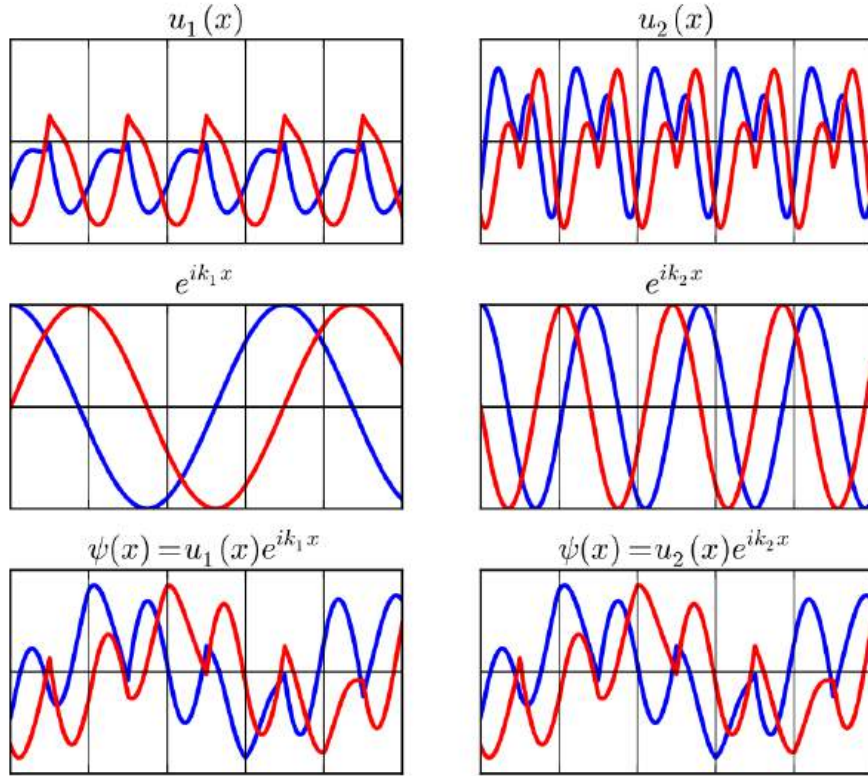**Figure 7.1:** Bloch Waves

The Bloch function (bottom) can be broken down as a product of a periodic function (top) and a plane wave (middle). The left and right plots represent the same Bloch state expressed in two different ways having two wave vectors k_1 and k_2 whose difference is the reciprocal lattice vector. Blue plots are real parts and red plots are imaginary plots of the Bloch function.

8
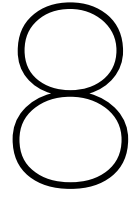
Density Of States

8.1. Definition

The DOS describes the number of available electronic modes or states per unit energy range. It is defined as $D(E) = N(E)/V$, where $N(E)$ is the total number of states in a system of volume V whose energy lies between E and $E + \delta E$,

$$D(E) = \int_{-\infty}^{\infty} g(E)f(E)\,dE$$

where $f(E)$ is the Fermi-Dirac distribution. It is a probability distribution, generally an average over the space and time domains of various states occupied by the state. The DOS, $D(E)$ varies as $\sqrt{E}$ near the Brillouin zone boundary. A high DOS for a particular energy level indicates that many states are available for occupation. DOS can be calculated for electrons, photons and phonons. Looking at the DOS for an electron at the bandgap between the valence and conduction band, an increase in electron energy makes more states available for occupation. An electron at the valence band edge must gain at least the bandgap energy of the material to transition to the conduction band.

DOS calculations are important as they allow us to predict the behaviour of materials. Understanding how electrons populate energy levels at different temperatures allows us to determine electrical conductivity, optical behaviour, and thermal properties. The DOS near the Fermi level, the highest occupied energy level at absolute zero, is particularly important in understanding the electronic behaviour of materials. It also provides insight into band structure indicating energy bands and bandgaps.

Pristine Graphene Supercell

9.1. Why Graphene?

Graphene is an allotrope of carbon made up of a single layer of hexagonally arranged sp^2 hybridised carbon atoms which forms the building block for higher dimensional allotropes like carbon nanotubes and fullerenes. Each atom in graphene is connected to 3 neighbours via a single σ bond and a delocalised π bond. This π bond delocalisation contributes to the valence band which extends over the whole sheet. In 2004, Andre Geim and Konstantin Novoselov isolated and examined the properties of "atomically thin carbon films" for which they were awarded the 2010 Nobel Prize in Physics[15].

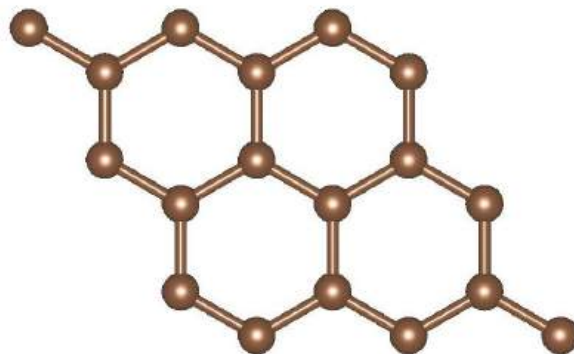**Figure 9.1:** Structure of a Pristine Graphene 3x3 Supercell

Pristine graphene is a zero-gap semiconductor with a point-like Fermi surface. The zero bandgap property makes graphene uninteresting from a device application view point. Graphene also has excellent electrical conductivity. One can always dope or alloy the simple graphene unit cell or supercell with elements like boron or nitrogen

which have very similar atomic masses compared to carbon which would be nice and snug fit. We shall explore the semiconducting graphene in upcoming chapters. Following are the properties computed for a 3×3 graphene supercell with 18 C atoms.

9.2. Density of States Calculation

Like mentioned earlier, graphene is a zero-gap semiconductor which translates to 0 DOS at the Fermi level which is at 0 eV.

1. Electronic Structure

   • The energies near 0 eV have vanishingly small DOS and the electronic structure is characterised by Dirac cones near the K and K′ points in the Brillouin zone.

   • Near these points, the dispersion is linear, $E(k) \propto \pm v_F|k|$ where v_F is the Fermi velocity.
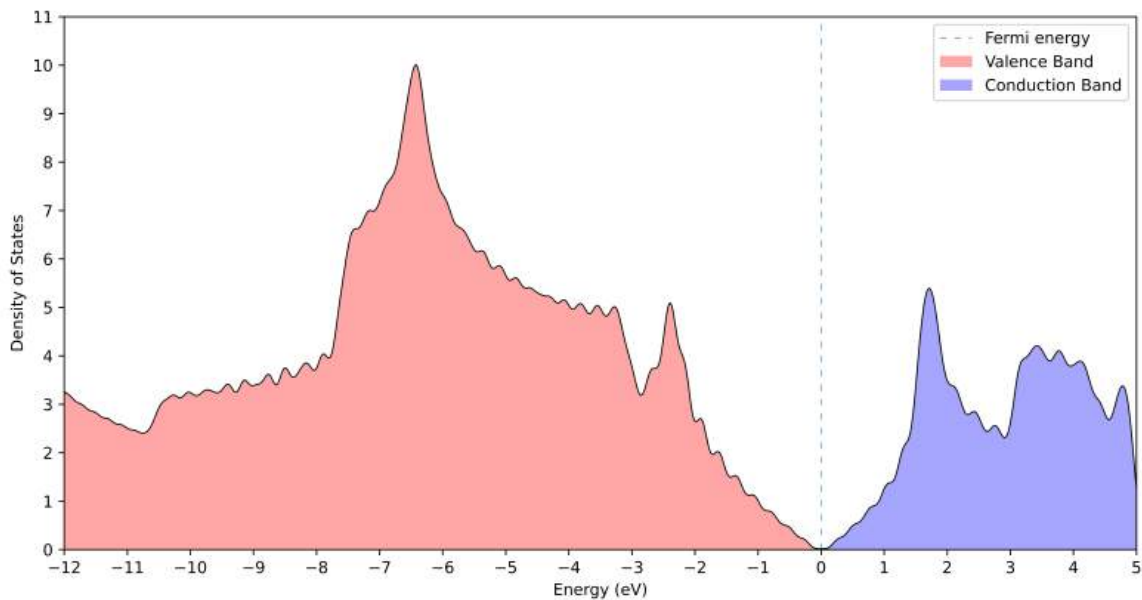

Figure 9.2: Density of States in a Pristine Graphene Supercell

2. Projected Density of States

   • **s-Orbital Contribution:** The s-orbital in graphene contributes primarily to the lower energy states, deep below the Fermi level.

   • **p-Orbital Contribution:** The p-orbitals, particularly the p_z orbitals, form the π and π^* bands in graphene. These bands are responsible for the linear dispersion near the Dirac points and dominate the DOS near the Fermi level as can be seen in Figure 9.3

9.3. Band Structure Calculation

By looking at the band structure of graphene in Figure 9.4, one can conclude that
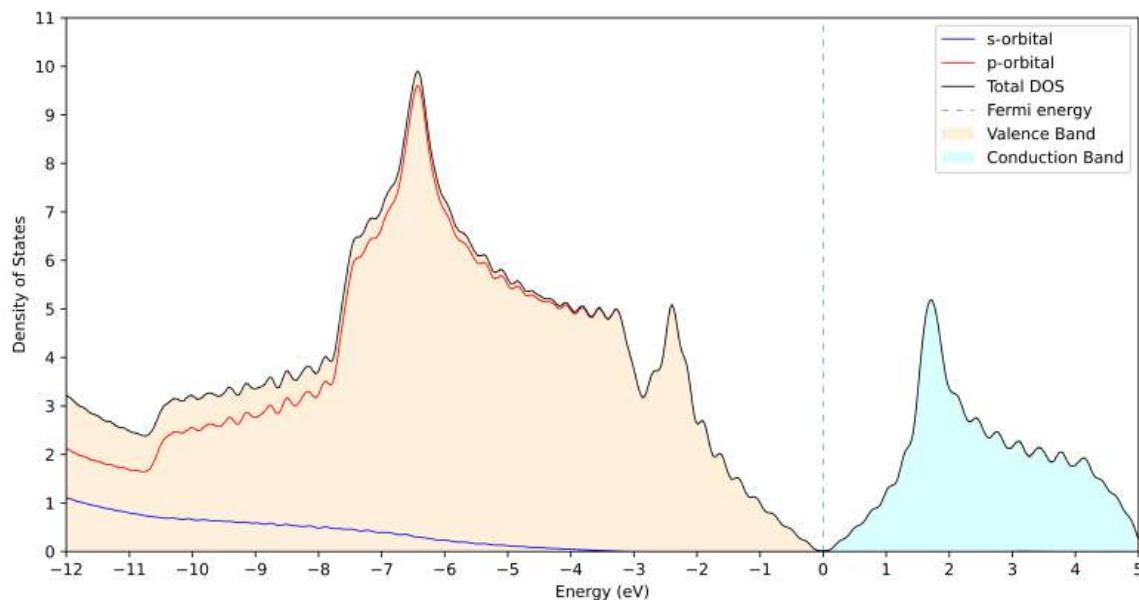
Figure 9.3: Projected DOS in a Pristine Graphene Supercell

1. High Symmetry Points

    (a) Since graphene is a 2-D material, it has 3 interesting high symmetry points: Γ, the centre of the Brillouin zone, M, the mid-point of the edge of the Brillouin zone, and K, one of the corners of the hexagonal Brillouin zone where the Dirac points are located.

2. Energy Bands

    • The Π and Π* bands form conical shapes near K and K′ points leading to the formation of the Dirac cone.

    • The σ bands are located much lower than the Fermi level and contribute less to the electronic properties near the Fermi level.

3. Absence of Bandgap

    • The absence of a bandgap imply that the conduction and valence bands meet at the Dirac point and thus gives graphene a metallic behaviour. This is also the reason for graphene's excellent electrical conductivity.

4. Angle-resolved photoemission Spectroscopy (ARPES) and scanning tunnelling spectroscopy (STS) are two powerful experimental techniques which measure the electronic band structure of materials. The results obtained computationally also match with ARPES and STS data.
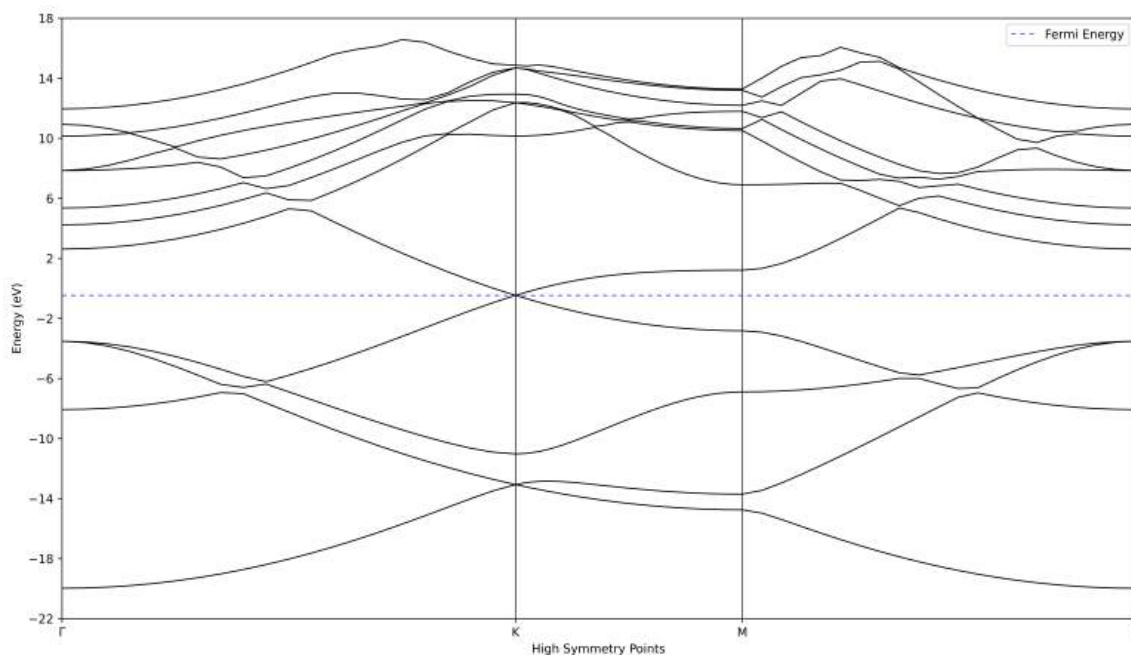
Figure 9.4: Bandstructure of a Pristine Graphene Supercell

9.4. Computational Details

7 programmes were run: `vc-relax`, `relax`, `scf`, `nscf`, `dos`, `projwfc`, and `bands`.[1]. A 10×10×1 grid was used for `vc-relax`, `relax`, and `scf`. The grid density was doubled for `nscf`. A `mixing_beta` of 0.4 was used for all programmes and `gaussian` smearing was used with a `degauss` value of `0.01`. Smearing, based on the `degauss` value allows the electrons a finite amount of time to be in a particular state before calculating the DOS. This may be useful in calculating the DOS for highly energetic molecules. The total CPU time was `9 hours 2 minutes` on the HPC cluster.

---

[1]More details about all the programmes can be found here `https://www.quantum-espresso.org/documentation/package-specific-documentation/`.

10

Boron Doped Graphene Supercell

10.1. What Changes When Graphene Is Doped With Boron?

As pointed out earlier, the boron atom is very likely to adjust to surrounding C atoms of the host as seen in Figure 10.1. After doping, the boron atom also undergoes sp^2 hybridisation and due to nearly same size of C and B, no significant distortion of the 2-D graphene is seen. Since B is smaller than C, the bond length C–B would be larger than C–C. This is in fact what I observed computationally. Compared to the previous C–C bond length of 1.4289Å, the C–B bond length is 1.502Å. This is a very good confirmation of the theory stated so far [17].
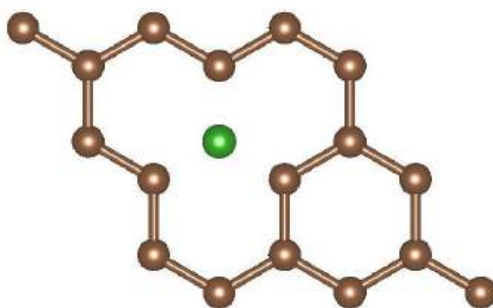

Figure 10.1: Structure of a Boron Doped 3x3 Graphene Supercell

10.2. Density of States Calculation

Boron being a group 13 element has the electronic configuration $[He]2s^2 2p^1$. It has one less electron than carbon and thus forms a p-type alloy with graphene.

1. Fermi Shift

   - Due to the electron deficiency of B, the Fermi energy shifts significantly by about 1.2 eV below the Dirac point.
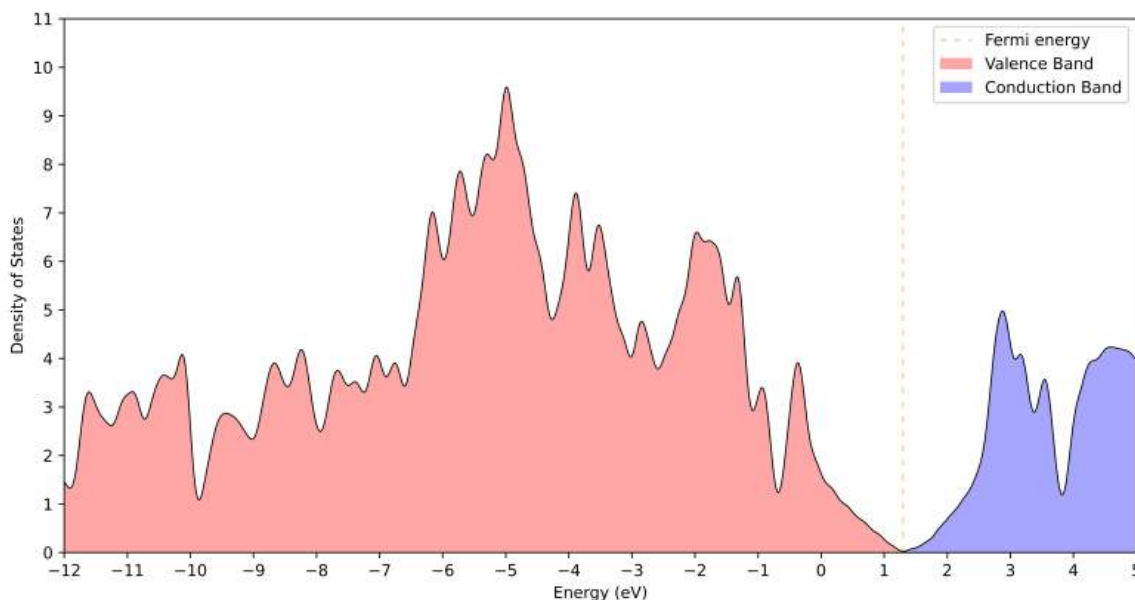

Figure 10.2: Density of States in a Boron-Doped Graphene Supercell

2. Nature of Boronated Graphene

   - Boronated graphene is no more a semi-metal. An energy gap of about 0.2 eV can be seen in the band structure (see Figure 10.4). This changes the behaviour of graphene from semi-metal to conductor.

3. Projected Density of States

   - PDOS calculations for boronated graphene reveal that the boron contribution is very minimal to non-existent. Since the concentration of doping is 5.56%, this result is expected.

   - **s-Orbital Contribution:** The C s-orbital contributes to the DOS towards the lower energies and does not contribute at all close to the Fermi level. Similar is true for B s-orbital whose contribution is even lower than C.

   - **p-Orbital Contribution:** The C p-orbital is the one which is contributing maximum to the DOS. It is significant even at low energies. Though B p-orbital does not contribute as much as C's, it still contributes a lot more than B s-orbital.

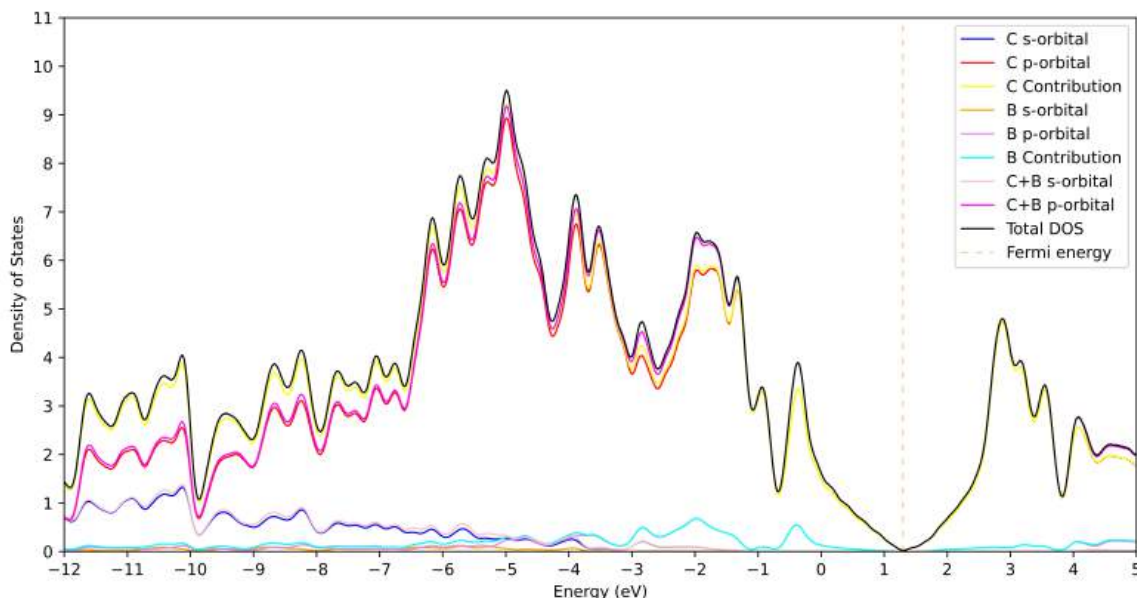   - All the contributions are zero at the Fermi level.

Figure 10.3: Projected DOS in a Boron Doped Graphene Supercell

10.3. Band Structure Calculation

1. High Symmetry Points

   - Boronated graphene also has the same 3 high symmetry points as pristine graphene did: Γ, M and K.

2. Energy Bands

   - There is a shift in the Fermi energy due to the presence of Boron. The Fermi energy is now around +1.2 eV.

3. Bandgap

   - As pointed out earlier, there is a gap in energy of about 0.2 eV at the Dirac points. The Dirac cones do not meet any more and thus gives boronated graphene a metallic character.

10.4. Computational Details

7 programmes were run: `vc-relax`, `relax`, `scf`, `nscf`, `dos`, `projwfc`, and `bands`.[1]. A 10×10×1 grid was used for `vc-relax`, `relax`, and `scf`. The grid density was doubled for `nscf`. A `mixing_beta` of 0.4 was used for all programmes and `gaussian` smearing was used with a `degauss` value of `0.01`. The total CPU time was `11 hours 28 minutes` on the HPC cluster.
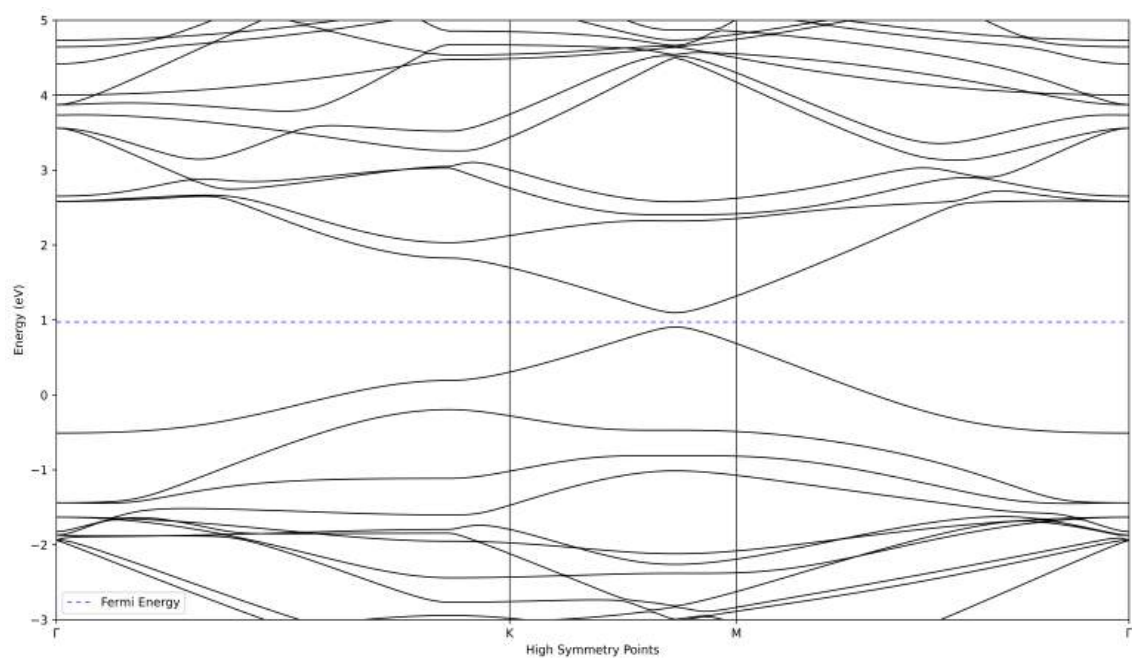
---

[1]More details about all the programmes can be found here `https://www.quantum-espresso.org/documentation/package-specific-documentation/`.

Figure 10.4: Band Structure of a Boron Doped Graphene Supercell

<div style="text-align: right;">

11

</div>

Nitrogen Doped Graphene Supercell

11.1. What Changes When Graphene Is Doped With Nitrogen?

The nitrogen atom is very likely to adjust to surrounding C atoms of the host as seen in Figure 11.1. After doping, the nitrogen atom also undergoes sp^2 hybridisation and due to nearly the same size of C and N, no significant distortion of the 2-D graphene is seen. Since N is larger than C, the bond length C–N would be smaller than C–C. This is in fact what I observed computationally. Compared to the previous C–C bond length of 1.4289Å, the C–N bond length is 1.4097Å. This is a very good confirmation of the theory stated so far [17].
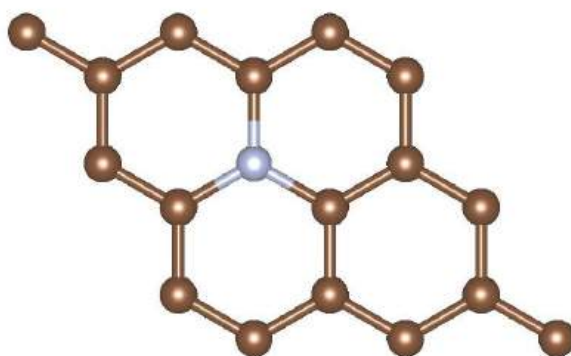

Figure 11.1: Structure of a Nitrogen-Doped 3x3 Graphene Supercell

11.2. Density of States Calculation

Nitrogen being a group 15 element has the electronic configuration $[He]2s^2 2p^3$. It has one more electron than carbon and thus forms a n-type alloy with graphene.

1. Fermi Shift

   - Due to the electron excess of N, the Fermi energy shifts significantly by about 1.1 eV above the Dirac point.
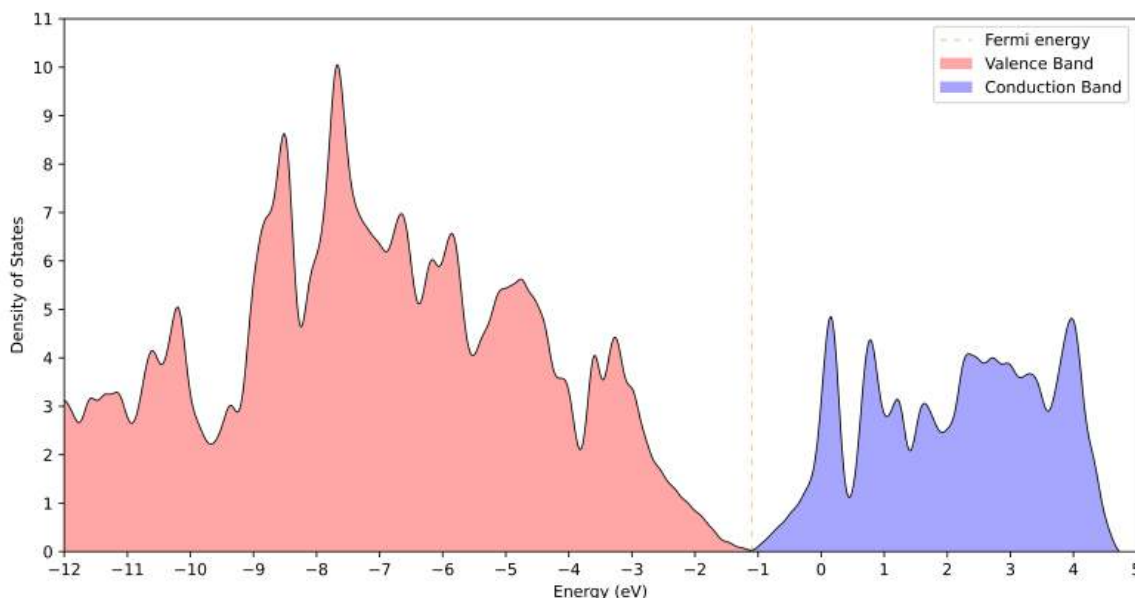

Figure 11.2: Density of States in a Nitrogen-Doped Graphene Supercell

2. Nature of Nitrogenated Graphene

   - Nitrogenated graphene is no more a semi-metal. An energy gap of 0.15 eV can be seen in the band structure (see Figure 10.4).

3. Projected Density of States

   - PDOS calculations for Nitrogenated graphene reveal that the nitrogen contribution is very minimal to non-existent. Since the concentration of doping is 5.56%, this result is expected.

   - **s-Orbital Contribution:** The C s-orbital contributes to the DOS towards the lower energies and contributes very minimally close to the Fermi level. Similar is true for N s-orbital whose contribution is even lower than C.

   - **p-Orbital Contribution:** The C p-orbital is the one which is contributing maximum to the DOS. It is significant even at low energies. Though N p-orbital does not contribute as much as C's, it still contributes a lot more than N s-orbital.

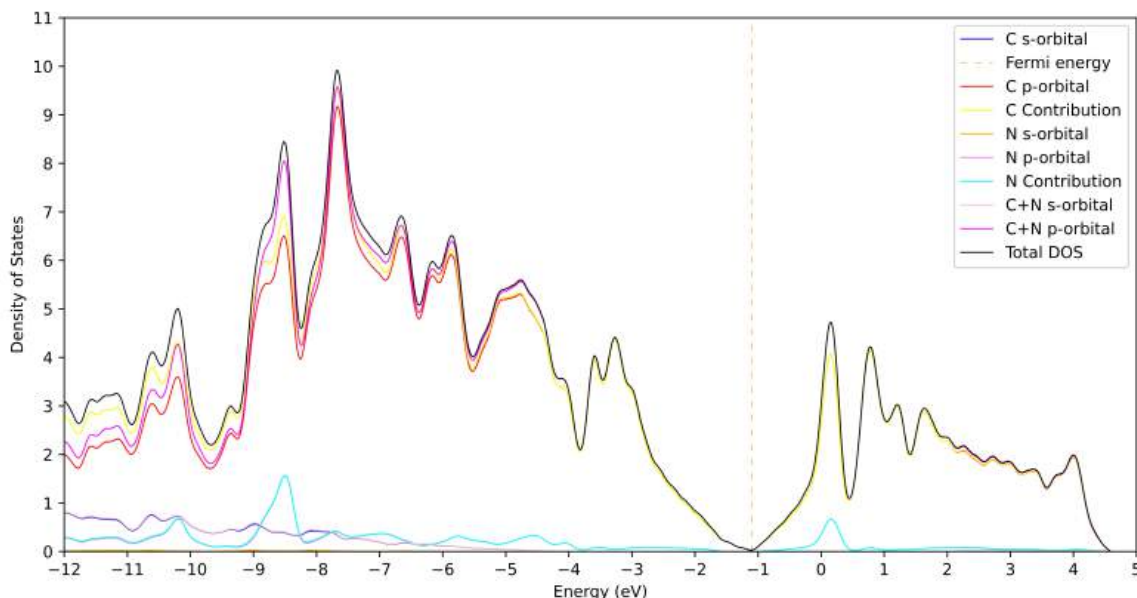   - All the contributions are zero at the Fermi level.

Figure 11.3: Projected DOS in a Nitrogen-Doped Graphene Supercell

11.3. Band Structure Calculation

1. High Symmetry Points

   - Nitrogenated graphene also has the same 3 high symmetry points as pristine graphene and boronated graphene: Γ, M and K.

2. Energy Bands

   - There is a shift in the Fermi energy due to the presence of Nitrogen. The Fermi energy is now around -1.1 eV.

3. Bandgap

   - As pointed out earlier, there is a gap in energy of 0.15 eV at the Dirac points. The Dirac cones do not meet any more and thus gives Nitrogenated graphene a metallic character.

11.4. Comparison of Different Types of Graphene

Figure 11.5 summarises the DOS of pristine, boronated and nitrogenated graphene. It is very clear that the nitrogenated graphene has a shift of about 1.1 eV to the left of the Fermi level of pristine graphene and boronated graphene has a shift of 1.2 eV to the right.

11.5. Computational Details

7 programmes were run: `vc-relax`, `relax`, `scf`, `nscf`, `dos`, `projwfc`, and `bands`.[1]. A 10×10×1 grid was used for `vc-relax`, `relax`, and `scf`. The grid density was doubled

---

[1]More details about all the programmes can be found here https://www.quantum-espresso.org/documentation/package-specific-documentation/.
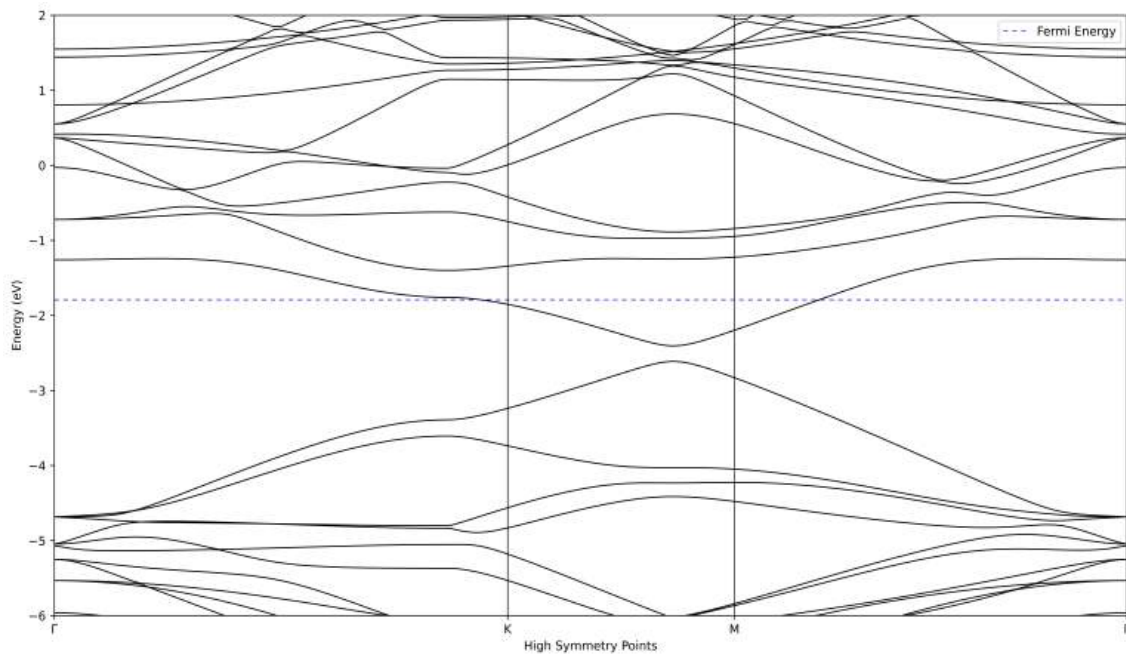
Figure 11.4: Band Structure of a Nitrogen-Doped Graphene Supercell

for `nscf`. A `mixing_beta` of 0.4 was used for all programmes and `gaussian` smearing was used with a `degauss` value of `0.01`. The total CPU time was `12 hours 2 minutes` on the HPC cluster.
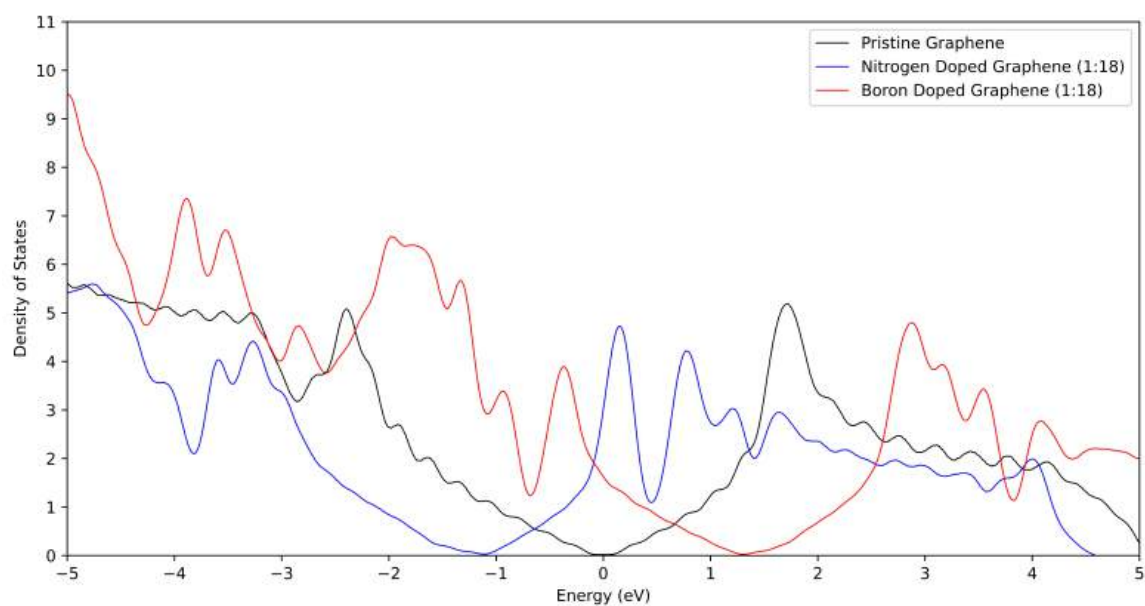
Figure 11.5: DOS Comparison in Pristine, Boronated and Nitrogenated Graphene Supercells

<div align="right">

12

</div>

<div align="right">

Silicon

</div>

12.1. Why Silicon?

Silicon is a tetravalent element of the carbon family and is a very good semiconductor. This is because of its inherent band gap which can be exploited in devices like solar cells, transistors and integrated circuits. In the ground state, it has the electronic configuration $[Ne]3s^2 3p^2$ and thus obtains the octet configuration by sp^3 hybridising. It has been well documented that Si crystallises in a diamond cubic crystal structure as seen in Figure 12.1. It is also possible to construct silicene, the silicon analogue of graphene.

Figure 12.1: Tetrahedral Structure of a Silicon Crystal

12.2. Density of States Calculation

Silicon being a semiconductor has a very unique DOS plot compared to graphene as it has a specific distribution of electronic states due to its crystal structure and electronic band structure.

1. Valence and Conduction Bands

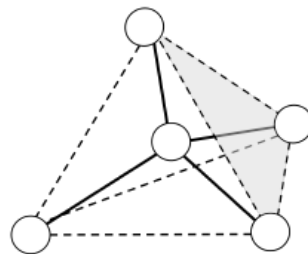   - **Valence Band:** The valence band is primarily composed of p-orbital states from silicon atoms. The density of states increases near the band edge and peaks before dropping off deeper into the band.

   - **Conduction Band:** The conduction band is primarily composed of s-orbital and p-orbital states. The density of states in the conduction band also increases from the band edge but differently compared to the valence band as seen in Figure 12.3.
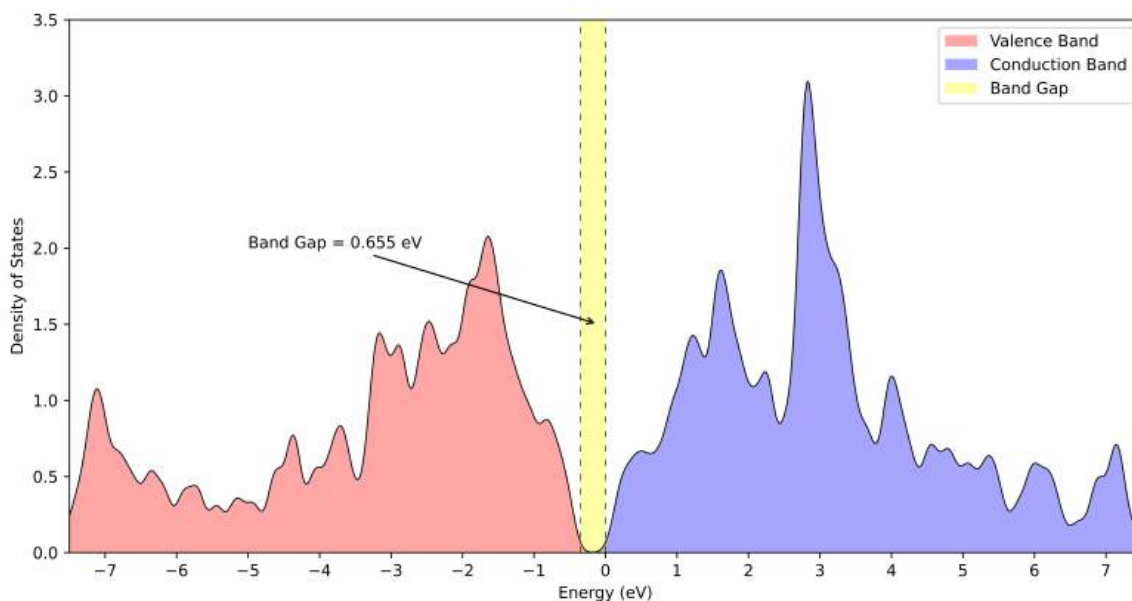
Figure 12.2: Electronic Density of States in a Silicon Crystal

2. Band Gap

   - Silicon has a band gap of 1.1 eV [13] which means that there are no electronic states available in the band gap. The electron in the valence band must gain at least the energy of the band gap to find itself in the conduction band.

   - The band gap obtained using PBE functional is around 0.655 eV. It is well known that PBE functional severely underestimates the band gap of certain systems, including silicon. For more accurate results, HSE or B3LYP functionals can be used which estimate the band gap much closer to the experimental values.

3. Projected Density of States

   - **s-Orbital Contribution:** The s-orbital contributes mainly to the lower part of the valence band. The s-states are typically located deeper in energy compared to the p-states.

   - **p-Orbital Contribution:** The p-orbitals are primarily responsible for the bonding in silicon and thus contribute significantly to the valence band

states. The p-orbital states are more dominant near the top of the valence band and also contribute to the conduction band states.

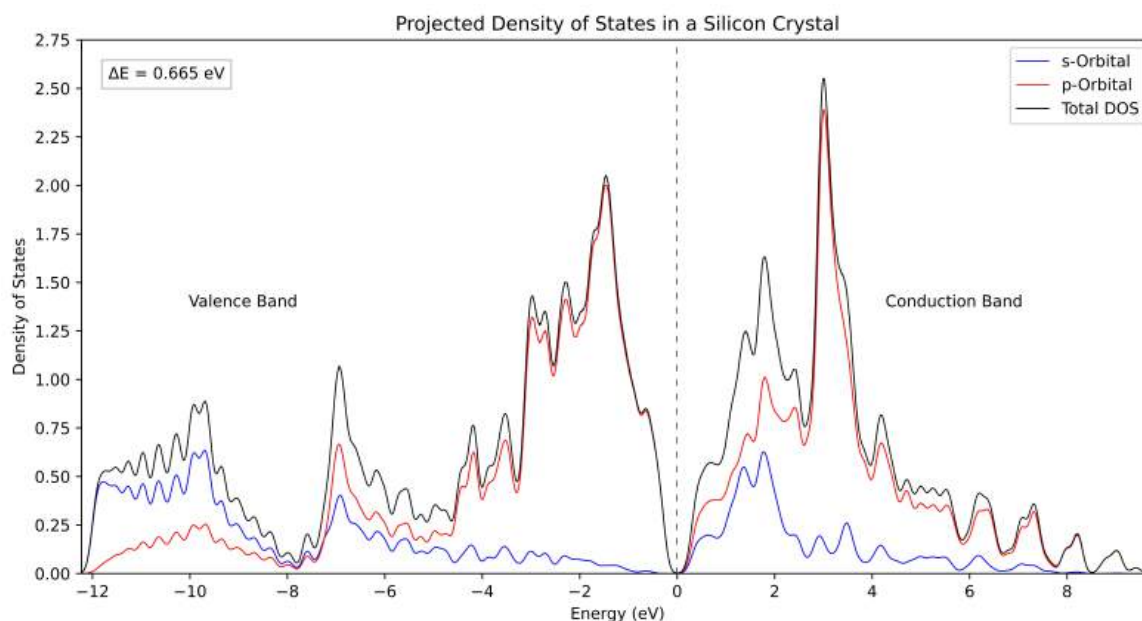**Figure 12.3:** Electronic Projected DOS in a Silicon Crystal

12.3. Band Structure Calculation

Silicon has an indirect bandgap, which means that the maximum energy of the valence band and the minimum energy of the conduction band occur at different places in the Brillouin zone.

1. Brillouin Zone

    (a) Silicon crystallizes in the diamond cubic structure, which corresponds to the face-centred cubic (FCC) Brillouin zone. Key points in this Brillouin zone include Γ (the centre), X, L, and K points.

2. Indirect Bandgap

    - The conduction band minimum occurs near the X point, while the valence band maximum is at the Γ point. The energy difference between these two points constitutes the indirect band gap, which is approximately 1.1 eV at room temperature. (Calculated value is close to 0.7 eV.)

3. Energy Dispersion

    - **Valence Band:** The valence band has its maximum at the Γ point, and the energy decreases as we move away from Γ to other points in the Brillouin zone.

    - **Conduction Band:** the conduction band minimum is near the X point. The energy increases as we move from the X point to the Γ point.
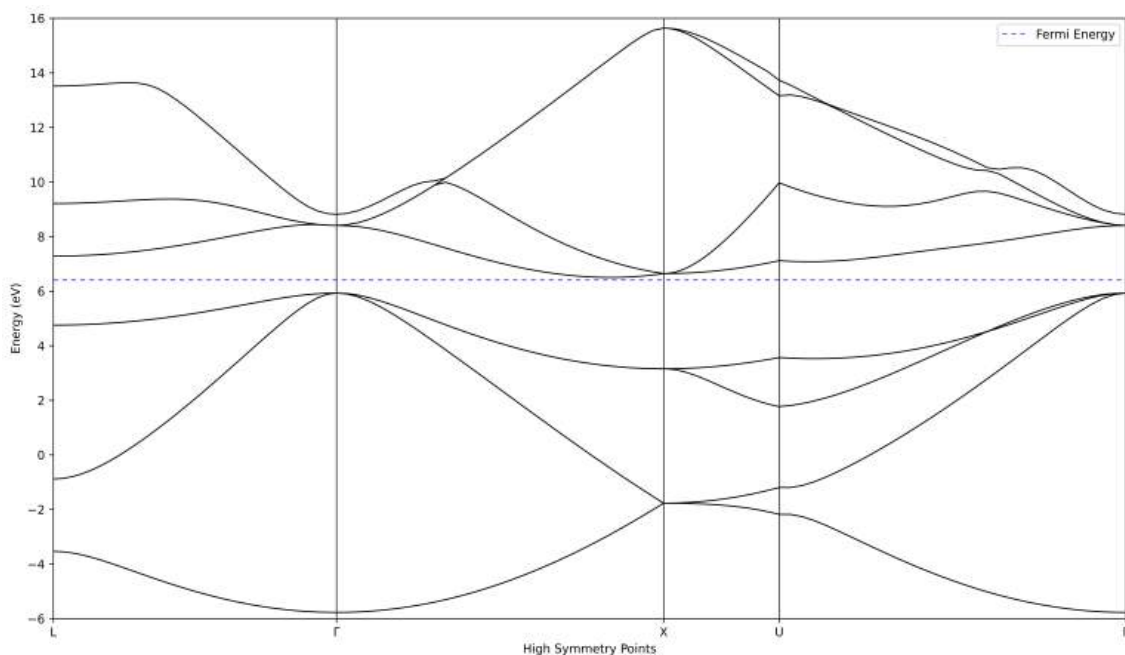
Figure 12.4: Bandstructure of a Silicon Crystal

12.4. Phonon Calculations

The phonon density of states in any crystal describes the number of phonon states per unit frequency (or energy) that are available for phonons (quantized vibrational modes) to occupy. This relationship is key to understanding the vibrational modes of the crystal which is useful in predicting its thermal and mechanical properties.

1. Phonon Dispersion Relations

   - In a crystalline solid like silicon, atoms vibrate around their equilibrium positions, and these vibrations can be described by phonon modes. Phonon modes are characterized by their wave vector **k** and branch index s, leading to a phonon dispersion relation $\omega_s(\mathbf{k})$, where ω is the phonon frequency.

2. Phonon Branches

   - Silicon has three acoustic and optical phonon branches each having one longitudinal and two transverse modes. Acoustic phonons have frequencies that approach zero as the wave vector approaches zero, while optical phonons have non-zero frequencies at the Brillouin zone centre. In Figure 12.5, there is a sharp peak at 490 cm^{-1}. The first-order Raman peak of silicon is at 520.2 cm^{-1}[16]. The computed value of the Raman peak is within 6% of the experimental value.

The phonon dispersion in a crystal gives the relationship between phonon frequencies and their corresponding wave vectors within the crystal's Brillouin zone. Like phonon DOS, this is also used to understand the mechanical properties of the crystal.
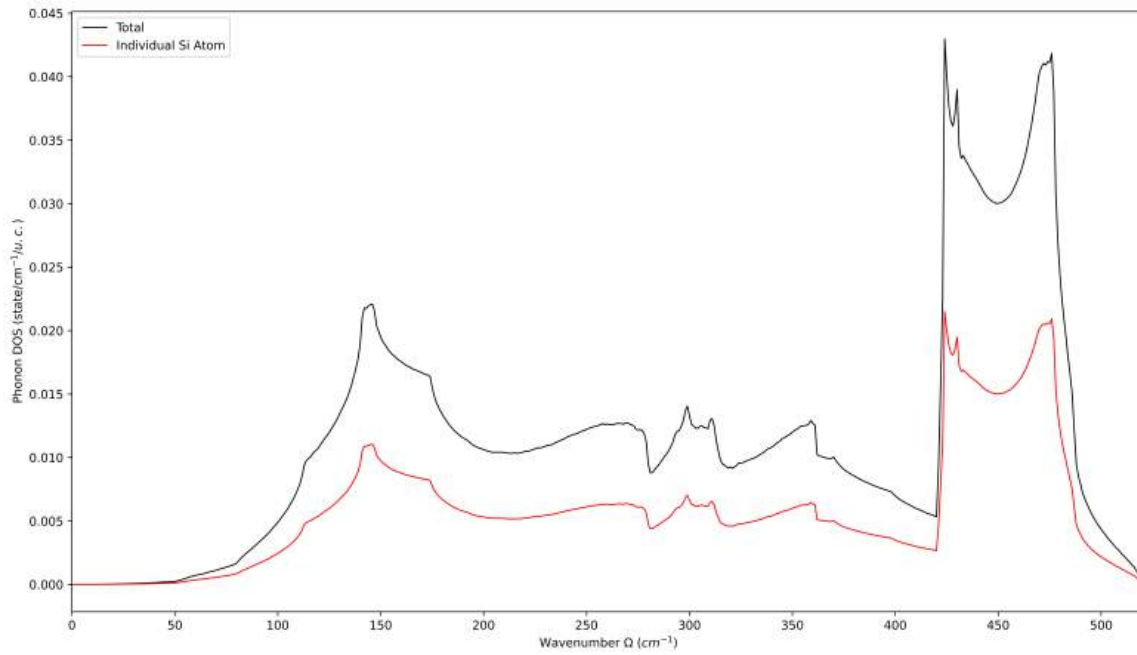
1. Phonon Modes

Figure 12.5: Phonon Density of States in a Silicon Crystal

- **Acoustic Phonons:** These phonons have atoms vibrating in phase with each other (similar to sound waves) and have both transverse and longitudinal modes.

- **Optical Phonons:** These phonons have atoms vibrating out of phase with each other (similar to electromagnetic waves) and have both transverse and longitudinal modes.

2. High-symmetry Points

- **Γ to X:** This direction shows the splitting of the acoustic and optical branches and provides information about the energy gap between these modes.

3. Experimental Techniques

- Experimental techniques like inelastic neutron scattering, Raman spectroscopy, and IR absorption are employed to investigate the phonon properties of silicon.

12.5. Computational Details

9 programmes were run: `vc-relax`, `relax`, `scf`, `nscf`, `dos`, `projwfc`, `bands`, `q2r`, and `matdyn`[1]. A 10×10×5 grid was used for `vc-relax`, `relax`, and `scf`. The grid density was doubled for `nscf`, `q2r` and `matdyn`. A `mixing_beta` of 0.4 was used for all programmes and the total CPU time was `19 minutes 46.34s` on the HPC cluster.

---

[1]More details about all the programmes can be found here `https://www.quantum-espresso.org/documentation/package-specific-documentation/`.
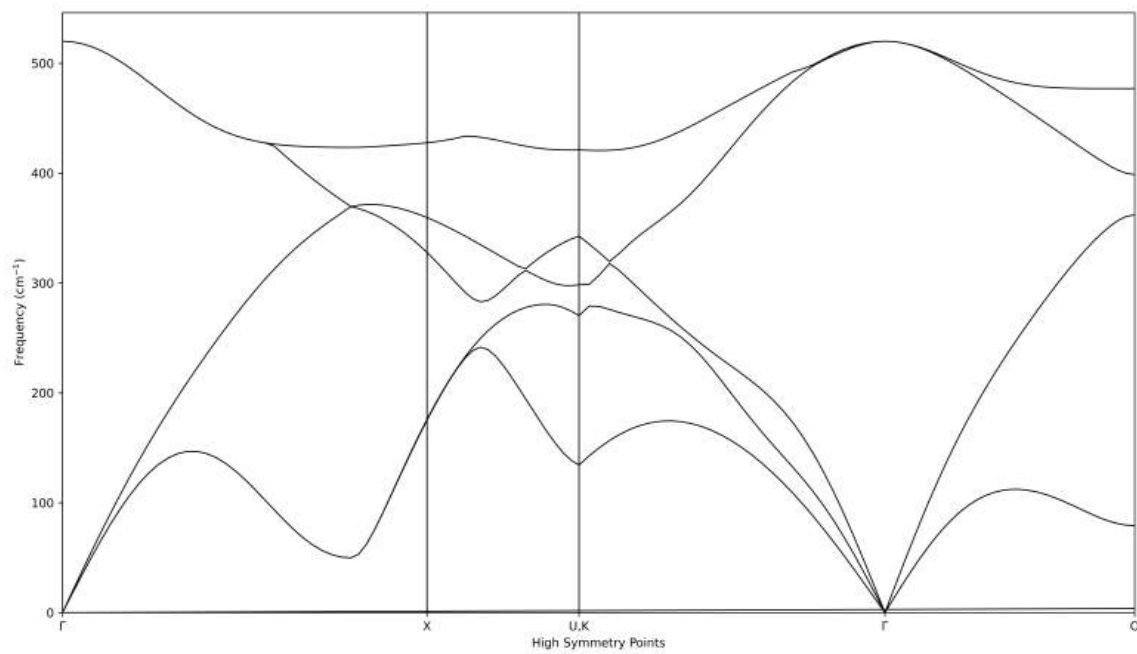
Figure 12.6: Phonon Dispersion in a Silicon Crystal

Water

13.1. Chemical Properties of Water

Using Quantum ESPRESSO, one can very accurately determine the chemical properties of the H_2O molecule. It is well known that the bond length of water (distance from one hydrogen to the oxygen) is 0.9584 Å [12]. It is also well known that the bond angle of the water molecule, an sp^3 hybridised entity which has a bent structure, is 104.45° [12]. The result is summarised below:

Parameter	Experimental Value		Calculated Value		Error
Bond Length	0.9584	Å	0.9756	Å	+1.79%
	1.811	Bohr	1.8436	Bohr	
Bond Angle	104.45	degrees	104.10	degrees	-0.34%

Table 13.1: Summary of calculated quantitative properties of water
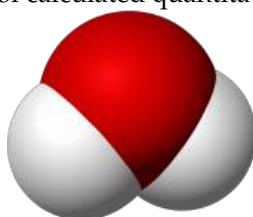
Figure 13.1: Space Filling Model of Water Molecule

13.2. Computational Details

4 programmes were run: `vc-relax`, `relax`, `scf`, and `nscf`. For the `vc-relax` and `relax` calculations, a comfortable 1×1×1 grid point was used since it uses very little computational resources and gives a very accurate result. For the `scf` calculation, a 10×10×1 grid point was used with `mixing_beta` of 0.4. The grid point density was changed to 20×20×1 for the `nscf` calculation and the output file of the nscf calculation

was opened in XCrySDen which calculated the bond angle and bond length. The total CPU time was `2 minutes 34.12s`.

14

Hydrogen

14.1. Chemical Properties of Hydrogen

The hydrogen molecule is the simplest molecule one could think of. The bond length of the hydrogen molecule is experimentally found to be 0.7414 Å[1] and has a dissociation energy of 430.53 kJ/mol. The same parameters were obtained computationally and the results are summarised in Table 14.1.

Parameter	Experimental Value		Calculated Value		Error
Bond Length	0.7414	Å	0.7495	Å	+1.09%
	1.4010	Bohr	1.4164	Bohr	
Dissociation Energy	430.53	kJ/mol	431.646	kJ/mol	+0.26%
	4.4624	eV/molecule	4.4736	eV/molecule	
	0.32978	Ry/molecule	0.32883	Ry/molecule	

Table 14.1: Summary of calculated quantitative properties of hydrogen

14.2. Computational Details

Only two programmes were run: `relax` and `scf`. For the `scf` calculation, the distance between the two hydrogen atoms was set to 3Å. `relax` calculation gives the optimised distance between the two hydrogen atoms. The difference between the total energy of the `relax` calculation and the `scf` calculation is the dissociation energy. A comfortable 3×3×1 grid point was used and the total CPU time was `10.36s`.

---

[1]The experimentally obtained values are taken from the NIST database `https://cccbdb.nist.gov/exp2x.asp?casno=1333740`.

Ammonia

15.1. Chemical Properties of Ammonia

Ammonia is an inorganic compound with a very simple structure. It has one nitrogen and three hydrogens arranged in a trigonal bipyramidal shape. The expected tetrahedral bond angle of 109°28′ is not observed because of the nitrogen lone-pair electron repulsion. The lone-pair repulsion is significantly stronger than the bond-pair repulsion which causes the hydrogens to move "inward" slightly. Thus, the experimentally observed bond angle is 106.7°. The N-H bond length is experimentally observed to be 1.0124 Å. Using DFT, the same parameters can be calculated computationally. Table 15.1 summarises the results obtained. (The experimentally obtained values are taken from the NIST Database.)
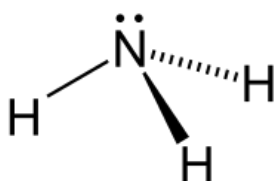
Figure 15.1: Stereo Structural Formula of Ammonia Molecule

Parameter	Experimental Value		Calculated Value		Error
Bond Length	1.0124	Å	1.0227	Å	+1.02%
	1.9132	Bohr	1.9326	Bohr	
Bond Angle	106.670	degrees	106.612	degrees	-0.05%

Table 15.1: Summary of calculated quantitative properties of ammonia

15.2. Pyramidal Inversion of Ammonia

Pyramidal or umbrella inversion is a fluxional process in which compounds with pyramidal structure turns "inside out" like an umbrella opened the wrong way on a gusty day. It is a rapid process in which the molecule or the ion passes through a

planar transition state. This allows for chiral molecules with a stereocentre to racemise. The inversion of ammonia at room temperature is very rapid, inverting some 30 billion times a second. Three key factors contribute to the rapidity: low energy barrier, narrow barrier width and low mass of hydrogen atoms. Experimentally, the inversion barrier is found to be 2013.5 cm^{-1} or 0.2496 eV[5]. Using Quantum ESPRESSO's NEB calculations, I computed the inversion barrier to be at 1843.21 cm^{-1} or 0.2285 eV, which is within 8.5% of the actual value.
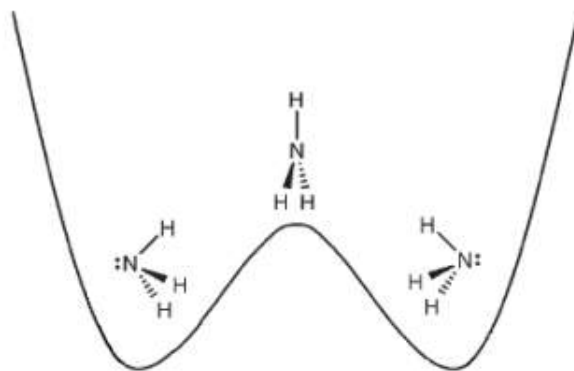
Figure 15.2: Pyramidal Inversion of Ammonia Molecule

15.3. Computational Details

3 programmes were run: `vc-relax`, `relax`, and `neb`[1]. For the `vc-relax` and `relax` calculations, a 5×5×5 grid point was used. For the `neb` calculation, a 10×10×10 grid point was used with `mixing_beta` of 0.4. The output file of the `relax` calculation was opened in XCrySDen which gave the bond length and bond angle while the output file of the `neb` calculation contained the value of the inversion barrier. The total CPU time was `5 minutes 46.09s`.

---

[1]More details can be found here `https://www.quantum-espresso.org/Doc/INPUT_NEB.html`.

<div style="text-align: right">

16

</div>

Pseudopotentials and Functionals

16.1. Pseudopotential Choice

As mentioned in section 6.5, pseudopotentials are simplifications of the actual complete potential an electron experiences in the crystal due to the other particles present. For computational purposes, there are many different types of pseudopotentials available to choose from. The Quantum ESPRESSO website[1] hosts a large collection of different pseudopotentials for nearly every element. One has to use different pseudopotentials depending on different calculation types. For heavier elements (which usually means anything which is not hydrogen) an FR pseudopotential is necessary for accurate calculations. A FR pseudopotential is also necessary when carrying out spin-orbit coupling calculations as the scalar relativistic approach does not give sufficient accuracy. Any calculation which has an element with Fe or heavier needs an FR input.

Among all the pseudopotentials, the most widely used are ONCV and US. ONCV is an instance of the norm-conserving pseudopotential which restricts that the total integrated electron density within r_c, the cutoff value usually of the order 10^{-8} to 10^{-10}, has to match all-electron electron density while the US relaxes this condition, thus requiring fewer plane waves to describe the pseudo-wavefunctions. ONCV inputs can not be given if one wishes to calculate the PDOS as Quantum ESPRESSO displays the error

```
Error in routine projwave (1):
Cannot project on zero atomic wavefunctions!
```

Another type of pseudopotential is the PAW. It expands the all-electron wavefunction within r_c of an atomic site $\mathbf{R}$ into a basis set of atomic wavefunctions $\Phi_u^{\mathbf{R}}$, called partial waves. The pseudo-wavefunctions are also expanded into a basis set of pseudo-partial waves $\Phi_u^{\mathbf{R}}$ which correspond to pseudised versions of the all-electron partial waves.

---

[1]This webpage hosts ready-to-use pseudopotentials taken from the PSLibrary `https://pseudopotentials.quantum-espresso.org/legacy_tables`.

There is no systematic manner for deciding which pseudopotential is 'better' as a pseudopotential that works well for obtaining one property may not work well for another property. In general, you would expect the PAW pseudopotential to be more accurate compared to the ultrasoft pseudopotential since the projector augmented waves should restore the pseudo-wavefunction up to the all-electron wavefunction behaviour, but this does not always guarantee that it would be more accurate than US or ONCV. The only way to truly determine which pseudopotential is 'best' for determining a specific material property is to benchmark the different pseudopotentials against the same property obtained from an all-electron DFT method on an example system as all of these pseudopotentials are trying to approximate it.

16.2. Functional Types

The default functional used for calculations in DFT is PBE as it is a non-empirical functional which has reasonable accuracy over a wide range of systems. It is based on GGA and while it is not the most accurate implementation of GGA, it is usually not too far off either. PBE underestimates the properties of certain molecules like band gap of Si and MoS_2. PBE's widespread use is also due to its relatively low computational demands compared to other hybrid functionals. The B3LYP, PBE0, HSE, and meta-hybrid GGA are all hybrid functionals.[20, 10]. B3LYP has terms which are based on GGA and LSDA while HSE uses an error function screened Coulomb potential to calculate the exchange portion of the interaction energy. While these functionals give extremely accurate results, the computational requirements are rather large, often several weeks which easily translates to years of CPU wall time on an HPC cluster!

References

[1] Enrico Fermi. "Motion of Neutrons in Hydrogenous Substances". In: *Ricerca Scientifica* 7 (June 1936), pp. 13–52.

[2] Enrico Fermi. "Statistical Method to Determine Some Properties of Atoms". In: *Rendiconti Lincei. Scienze Fisiche e Naturali* 22 (Dec. 2011), pp. 283–314.

[3] Vladimir A. Fock. "Näherungsmethode zur Lösung des quantenmechanischen Mehrkörperproblems". In: *Zeitschrift fur Physik* 61.1-2 (Jan. 1930), pp. 126–148. DOI: `10.1007/BF01340294`.

[4] Thomas L. Gilbert. "Hohenberg-Kohn Theorem for Nonlocal External Potentials". In: *Phys. Rev. B* 12 (6 Sept. 1975), pp. 2111–2120. DOI: `10.1103/PhysRevB.12.2111`. URL: `https://link.aps.org/doi/10.1103/PhysRevB.12.2111`.

[5] Arthur M. Halpern, B. R. Ramachandran, and Eric D. Glendening. "The Inversion Potential of Ammonia: An Intrinsic Reaction Coordinate Calculation for Student Investigation". In: *Journal of Chemical Education* 84.6 (2007), p. 1067. DOI: `10.1021/ed084p1067`. eprint: `https://doi.org/10.1021/ed084p1067`. URL: `https://doi.org/10.1021/ed084p1067`.

[6] John E. Harriman. "Orthonormal Orbitals for the Representation of an Arbitrary Density". In: *Phys. Rev. A* 24 (2 Aug. 1981), pp. 680–682. DOI: `10.1103/PhysRevA.24.680`. URL: `https://link.aps.org/doi/10.1103/PhysRevA.24.680`.

[7] Douglas R. Hartree. "The Wave Mechanics of an Atom with a Non-Coulomb Central Field. Part II. Some Results and Discussion". In: *Mathematical Proceedings of the Cambridge Philosophical Society* 24.1 (1928), pp. 111–132. DOI: `10.1017/S0305004100011920`.

[8] Douglas R. Hartree and W. Hartree. "Self-Consistent Field, with Exchange, for Beryllium". In: *Proceedings of the Royal Society of London Series A* 150.869 (May 1935), pp. 9–33. DOI: `10.1098/rspa.1935.0085`.

[9] Pierre Hohenberg and Walter Kohn. "Inhomogeneous Electron Gas". In: *Phys. Rev.* 136 (3B Nov. 1964), B864–B871. DOI: `10.1103/PhysRev.136.B864`. URL: `https://link.aps.org/doi/10.1103/PhysRev.136.B864`.

[10] K. Kim and K. D. Jordan. "Comparison Of Density Functional And MP2 Calculations On The Water Monomer And Dimer". In: *The Journal of Physical Chemistry* 98.40 (1994), pp. 10089–10094. DOI: `10.1021/j100091a024`. eprint: `https://doi.org/10.1021/j100091a024`. URL: `https://doi.org/10.1021/j100091a024`.

[11] Walter Kohn and Lu J. Sham. "Self-Consistent Equations Including Exchange and Correlation Effects". In: *Phys. Rev.* 140 (4A Nov. 1965), A1133–A1138. DOI: `10.1103/PhysRev.140.A1133`. URL: `https://link.aps.org/doi/10.1103/PhysRev.140.A1133`.

[12] I.N. Levine. *Quantum Chemistry*. Pearson advanced chemistry series. New York: Pearson, 2014. ISBN: 9780321890603. URL: `https://books.google.co.in/books?id=ht6jMQEACAAJ`.

[13] Jeremy Low et al. "Band Gap Energy In Silicon". In: *American Journal of Undergraduate Research* 7 (June 2008). DOI: `10.33697/ajur.2008.010`.

[14] Donald A. McQuarrie. *Statistical Mechanics*. Harper's Chemistry Series. New York: Harper Collins, 1976.

[15] K. S. Novoselov et al. "Electric Field Effect In Atomically Thin Carbon Films". In: *Science* 306.5696 (2004), pp. 666–669. DOI: `10.1126/science.1102896`. eprint: `https://www.science.org/doi/pdf/10.1126/science.1102896`. URL: `https://www.science.org/doi/abs/10.1126/science.1102896`.

[16] J. H. Parker, D. W. Feldman, and M. Ashkin. "Raman Scattering By Silicon And Germanium". In: *Phys. Rev.* 155 (3 Mar. 1967), pp. 712–714. DOI: `10.1103/PhysRev.155.712`. URL: `https://link.aps.org/doi/10.1103/PhysRev.155.712`.

[17] Pooja Rani and Vijay Jindal. "Designing Band Gap of Graphene by B and N Dopant Atoms". In: *RSC Advances* (Sept. 2012). DOI: `10.1039/C2RA22664B`.

[18] Peter Schwerdtfeger. "The Pseudopotential Approximation in Electronic Structure Theory". In: *ChemPhysChem* 12.17 (2011), pp. 3143–3155. DOI: `https://doi.org/10.1002/cphc.201100387`. eprint: `https://chemistry-europe.onlinelibrary.wiley.com/doi/pdf/10.1002/cphc.201100387`. URL: `https://chemistry-europe.onlinelibrary.wiley.com/doi/abs/10.1002/cphc.201100387`.

[19] John C. Slater. "Note on Hartree's Method". In: *Phys. Rev.* 35 (2 Jan. 1930), pp. 210–211. DOI: `10.1103/PhysRev.35.210.2`. URL: `https://link.aps.org/doi/10.1103/PhysRev.35.210.2`.

[20] P. J. Stephens et al. "Ab Initio Calculation Of Vibrational Absorption And Circular Dichroism Spectra Using Density Functional Force Fields". In: *The Journal of Physical Chemistry* 98.45 (1994), pp. 11623–11627. DOI: `10.1021/j100096a001`. eprint: `https://doi.org/10.1021/j100096a001`. URL: `https://doi.org/10.1021/j100096a001`.

[21] Edward Teller. "On the Stability of Molecules in the Thomas-Fermi Theory". In: *Rev. Mod. Phys.* 34 (4 Oct. 1962), pp. 627–631. DOI: `10.1103/RevModPhys.34.627`. URL: `https://link.aps.org/doi/10.1103/RevModPhys.34.627`.

[22] Llewellyn H. Thomas. "The Calculation of Atomic Fields". In: *Mathematical Proceedings of the Cambridge Philosophical Society* 23.5 (1927), pp. 542–548. DOI: `10.1017/S0305004100011683`.